



## 1. Introduction

Since the outbreak of the deadly COVID-19 in Wuhan, China, coronaviruses (CoVs) have become a major class of RNA viruses that induces respiratory, gastrointestinal, hepatic, and neurological diseases in humans and can also infect animals [1]. They were first identified in human embryonic tracheal organ cultures acquired from the respiratory tract of an adult with a common cold, in the mid-1960s [2]. In December 2019, a collection of local health authorities recorded batches of patients with the unclear cause of pneumonia that was related to the seafood market in Wuhan Province of Hubei, China [3]. The new pathogen, a novel coronavirus (SARS-CoV-2) was later identified using a mechanism of surveillance for "pneumonia of unknown etiology" [4].

There are currently no established antiviral medications or vaccinations, making it a critical threat to both persons and the economy. A thorough understanding of the nature of the pandemic is crucial to limiting infection. Numerous researchers have developed mathematical models for the spread of SARS-CoV-2 to gain insight into the disease's transmission dynamics, which may lead to its eradication. The majority of the models are based on classical differential equations. However, fractional-order differential equations outperform standard mathematical modeling [5]. It has achieved significance mainly because its applications can be found in various fields of science, engineering, finance, and epidemiology; see for example the recent results [6–9] and references cited therein.

The fractional-order differential equations (FODEs) models appear to be more reliable with real-world problems than the integer-order models. The fractional derivative concept was first proposed

by Riemann-Liouville. After that Caputo-Fabrizio in [10] proposed a new fractional derivative using the exponential kernel. This derivative has a few problems related to the locality of the kernel. The newly updated version of a fractional derivative was proposed by Atangana and Baleanu (AB) in [11] with the support of the Mittag-Leffler function (MLF) as nonsingular kernel and nonlocal. Several experiments on mathematical models via functional derivative were presented see [12, 13]. Mohammed et al. [14] have studied fourteen nonlinear FDEs applying the fractional Adams Bashforth (AB) method and later introduced the fractional nonlocal operator Atangana-Baleanu (AB) to understand more easily. The findings obtained by Mohammed et al. [14] play an important role in the formulation of the theory of fractional analytical dynamic for the ongoing pandemic due to COVID-19, which has seriously affected the whole world. Zizhen in [15] presented the approach of fractional differentiation to capture different memories including power law, decay and crossover behaviors. COVID-19 models using fractional derivatives were also considered in [16–19] and references therein. Figs. 1-5 shows the total number of cases, daily new cases, active cases, total deaths, and daily deaths due to COVID-19 as of 29 March, 2021 in Turkey [20]. In

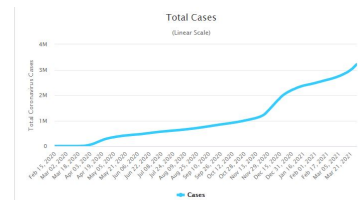


**Fig. 1.** Total COVID-19 Cases in Turkey as of 29 March, 2021.

this paper, we developed a mathematical

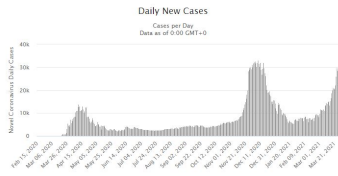


**Fig. 2.** Daily New Cases in Turkey as of 29 March, 2021.

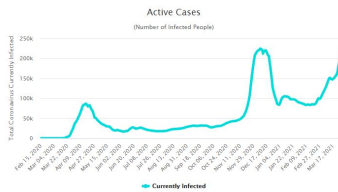


**Fig. 3.** Active Cases in Turkey as of 29 March, 2021.

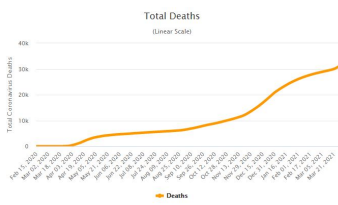


**Fig. 4.** Total Coronavirus Deaths in Turkey as of 29 March, 2021.

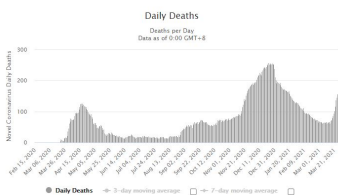


**Fig. 5.** Daily New Deaths in Turkey as of 29 March, 2021.

model including quarantine and asymptomatic compartment and later generalized to the fractional-order derivative in the Atangana-Baleanu context (ABC) and our findings lead to a deeper understanding of the COVID-19 pandemic transmission dynamics and provide valuable advice for the future design of control strategies.

The paper is structured as follows.

We formulate the model and study its stability analysis in Section 2. In Section 3, we transform the proposed model into the fractional-order differential equations in the setting of ABC-fractional operators and establish its existence and uniqueness of solutions using fixed point theorems. In Section 4, based on the real data of Turkey, we validate the proposed model and obtain the best parameters. Besides, using the Toefik-Atangana numerical scheme, we present the numerical results. In Section 5, we conclude the paper and present some discussion.

## 2. Model Formulation

Before building the model, let us presume that the population of humans denoted by  $N(t)$  may be divided into six subclasses: individuals who are susceptible  $S(t)$ , described as the group of humans, who might be infected by COVID-19. They can either be infected through direct, indirect (through infected items or surfaces) or close contact with infected people via mouth and nose secretions. Exposed individuals  $E(t)$ , asymptotically infected individuals  $A(t)$ , described as the group of humans who are already infected by COVID-19, while still at a non-harmful level. Humans may also perform everyday tasks like susceptible humans in this group. Transmission between asymptotically infected individuals with health could take place in the form of  $\eta \xi_{sa} SA$ , in which  $\eta$  is the infection probability and  $\eta \in [0, 1]$ . Quarantined individuals  $Q(t)$ , symptomatic infectious individuals (confirmed with infectious capacity)  $I(t)$ , and recovered cases (immune)  $R(t)$ . Thus, the total population  $N(t) = S(t) + E(t) + A(t) + Q(t) + I(t) + R(t)$ .

The transmission mechanism involving the six compartments above is seen in the diagram below. The recruitment rate

only exists in susceptible humans  $S(t)$  with a constant rate  $\Lambda$ . Each compartment drops due to the normal death rate  $\mu$  except for the infected human compartment  $I(t)$  where mortality caused by COVID-19 has a rate of  $\delta$ . Susceptible humans might be infected by direct contact with infected humans with the probability of infection  $\xi_{si}$  if they are infected by  $I(t)$  compartment,  $\xi_{sa}$  and  $\xi_{se}$  if they are infected by  $A(t)$  and  $E(t)$  compartments respectively. The incubation period was defined as  $\tau_1$ . Quarantined persons can be moved to the class of infected individuals with symptoms that develop at the rate of  $\alpha_2$  and proportion of  $\sigma_3$ . The parameter  $r_1, r_2, r_3$  indicates the recovery rate of infected individuals without symptoms (asymptomatic), quarantined individuals, and infected individuals with symptoms (symptomatic) to be shifted to recovered individuals class  $R$ .

Fig. 6, shows the illustrative transmission pattern of the COVID-19 proposed model while the meaning of each state variable, as well as the parameters associated with the proposed model, are given in Tables 1-2. Based on Fig. 6, we generate the

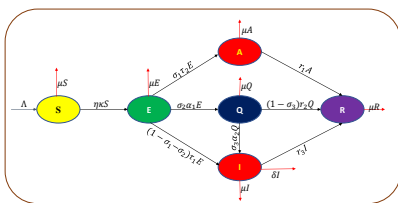


**Fig. 6.** Transmission of COVID-19 diagram.

following system of nonlinear differential equations given by:

$$\begin{aligned}\frac{dS}{dt} &= \Lambda - \eta\kappa S - \mu S, \\ \frac{dE}{dt} &= \eta\kappa S - (\sigma_1\tau_2 + \sigma_2\alpha_1 + \mu + \tau_1 - \sigma_1\tau_1 - \sigma_2\tau_1)E, \\ \frac{dA}{dt} &= \sigma_1\tau_2 E - (r_1 + \mu)A,\end{aligned}$$

$$\begin{aligned}\frac{dQ}{dt} &= \sigma_2\alpha_1 E - (\sigma_3\alpha_2 + r_2 - r_2\sigma_3 + \mu)Q, \\ \frac{dI}{dt} &= (1 - \sigma_1 - \sigma_2)\tau_1 E + \sigma_3\alpha_2 Q - (r_3 + \mu + \delta)I, \\ \frac{dR}{dt} &= r_1 A + (1 - \sigma_3)r_2 Q + r_3 I - \mu R,\end{aligned}\tag{2.1}$$

where  $\kappa = \frac{\xi_{se}E + \xi_{si}I + \xi_{sa}A}{N}$  and the initial condition:

$$\begin{aligned}S(0) &= S_0 \geq 0, E(0) = E_0 \geq 0, A(0) = A_0 \geq 0, \\ Q(0) &= Q_0 \geq 0, I(0) = I_0 \geq 0, R(0) = R_0 \geq 0.\end{aligned}\tag{2.2}$$

**Table 1.** Description of the state variables.

| Variables | Description                       |
|-----------|-----------------------------------|
| $S$       | Susceptible individuals           |
| $E$       | Exposed individuals               |
| $A$       | Asymptomatic infected individuals |
| $Q$       | Quarantine individuals            |
| $I$       | Symptomatic infected individuals  |
| $R$       | Recovery individuals              |

**Table 2.** Description of the parameters.

| Parameters | Description   |
|------------|---|
| $\Lambda$  | Recruitment of susceptible individuals                                    |
| $\mu$      | Natural mortality rate  |
| $\eta$     | Rate of transmission during contact                                       |
| $\xi_{se}$ | Contact rate between susceptible and exposed individuals                  |
| $\xi_{sa}$ | Contact rate between susceptible and asymptomatic infections individuals. |
| $\xi_{si}$ | Contact rate between susceptible and symptomatic infectious individuals   |

|            |   |
|------------|---|
| $\sigma_1$ | Proportion of asymptotically infected individuals   |
| $\sigma_2$ | Proportion of quarantined exposed individuals   |
| $\alpha_1$ | Movement rate of exposed individuals to quarantined individuals                             |
| $\tau_1$   | Rate of transmission after incubation period and transferred to symptomatic infected class  |
| $\tau_2$   | Rate of transmission after incubation period and transferred to asymptomatic infected class |
| $\alpha_2$ | Movement rate of quarantined individual to symptomatic infected individuals                 |
| $\sigma_3$ | Proportion of quarantined symptomatic infected individuals                                  |
| $r_1$      | Recovery rate of asymptotically infected individuals and transferred to R class             |
| $r_2$      | Recovery rate of persons in quarantine and moved to the R class                             |
| $r_3$      | Recovery rate of symptomatic infected individuals and transferred to R class                |
| $\delta$   | Mortality rate due to COVID-19  |

In general, population dynamics are obtained by summing up the five equations in the model (2.1) resulting in:

$$\frac{dN}{dt} = \Lambda - \mu N - \delta I.$$

The positive area of invariants that matches the model (2.1) is given by

$$\Omega = \left\{ (S(t), E(t), A(t), Q(t), I(t), R(t)) \in \mathbb{R}_+^6 : N(t) \leq \frac{\Lambda}{\mu} \right\}.$$

## 2.1 Stability analysis

The present section explores the stability for the model (2.1) by considering first the disease free equilibrium and the basic reproduction number denoted by  $R_0$ . The equilibrium point is acquired at

$$\frac{dS}{dt} = \frac{dE}{dt} = \frac{dA}{dt} = \frac{dQ}{dt} = \frac{dI}{dt} = \frac{dR}{dt} = 0. \quad (2.3)$$

Thus, from system (2.1), the disease-free equilibrium (DFE) point represented by  $E_{dfe}$ , is given by

$$E_{dfe} = (S_0, 0, 0, 0, 0, 0) = \left( \frac{\Lambda}{\mu}, 0, 0, 0, 0, 0 \right). \quad (2.4)$$

The basic reproduction number denoted by  $R_0$  is the predicted infection rate value per time unit. The infection is caused by an infectious person in a susceptible population. Hence,  $R_0$  is computed using the next generation matrix technique proposed in [21]. In view of system (2.1), the equation for  $R_0$  is given by

$$R_0 = o(\mathcal{F}\mathcal{V}^{-1}) = R_1 + R_2, \quad (2.5)$$

where

$$R_1 = \frac{\eta \xi_{se} (r_1 + \mu) + \eta \xi_{sa} \sigma_1 \tau_2}{(r_1 + \mu)(\mu + \tau_1 + \sigma_1 \tau_2 + \sigma_2 \alpha_1 - \sigma_1 \tau_1 - \sigma_2 \tau_1)},$$

$$R_2 = \frac{\xi_{si} \eta \sigma_3 \alpha_2 \alpha_1 \sigma_2 + q_1 \xi_{si} \eta (\tau_1 - \sigma_2 \tau_1 - \sigma_1 \tau_1)}{q_2 (\mu + \delta + r_3) (\mu + r_2 - r_2 \sigma_3 + \sigma_3 \alpha_2)},$$

$$\text{and } q_1 = \mu + r_2 - r_2 \sigma_3 + \sigma_3 \alpha_2, \quad q_2 = \mu + \tau_1 + \sigma_1 \tau_2 + \alpha_1 \sigma_2 - \sigma_1 \tau_1 - \sigma_2 \tau_1.$$

**Theorem 2.1.** *The disease-free equilibrium  $E_{dfe}$ , of the system (2.1) is locally asymptotically stable if  $R_0 < 1$ .*

## 3. Fractional-Order Coronavirus Model

The extension of integer order differential equations is fractional-order differential equations. At the end of the sixteenth century (1695), the concept of fractional calculus was introduced. Fractional derivatives are exceptional techniques for describing the general properties of various materials and processes due to nonlocal and memory behavior. Furthermore, fractional derivatives were considered to be effective and more reliable than classical derivatives in modeling various mechanical and electrical properties of real materials. There are different types

of fractional operators that are proposed by Riemann-Liouville, Caputo, Hadamard, Caputo-Fabrizio and so on. Recently, Atangana-Baleanu [22] introduced an interesting fractional operator called Atangana-Baleanu Caputo fractional operator (ABC). The operator is used as a global operator for the modeling of various processes and physical systems, which emerged in subjects like physics, dynamics, fluid mechanics, control theory, chemistry, mathematical biology, etc., the reader is recommended to [23, 24]. It is discovered that the operator can more effectively model real-world problems than integer-order cases. This operator has piqued the interest of many mathematicians and researchers due to its relevance and wide variety of applications.

Motivated by the aforementioned advantages, we generalize nonlinear differential equations (2.1) to nonlinear fractional differential equations in the form of the ABC fractional derivative. Furthermore, we have some fundamental facts and concepts. Based on these facts, we elaborate on our proposed fractional model.

**Definition 3.1** ([22]). The ABC-fractional integral of order  $\nu$  with the lower limit  $0^+$  for a function  $g$  is defined by

$${}^{ABC}I_{0^+}^\nu g(t) = \frac{1-\nu}{N(\nu)} + \frac{\nu}{N(\nu)} \frac{1}{\Gamma(\nu)} \int_0^t (t-x)^{\nu-1} g(x) dx,$$

where  $t, \nu > 0$  and  $\Gamma(\cdot)$  denotes the gamma function.

**Definition 3.2** ([22]). The ABC-fractional derivative of order  $0 < \nu \leq 1$  with the lower limit  $0^+$  for a function  $g$  is defined by

$${}^{ABC}\mathcal{D}_{0^+}^\nu g(t) = \frac{N(\nu)}{(1-\nu)} \int_0^t E_\nu \left( \frac{-\nu}{1-\nu} (t-x)^\nu \right) g'(x) dx,$$

provided the function  $g$  differentiable on  $[0, +\infty)$ , where  $\Gamma(\cdot)$  denotes the gamma function. Here the normalization function  $N(\nu)$  is given by  $N(\nu) = 1 - \nu + \frac{\nu}{N(\nu)}$  and  $N(0) = N(1) = 1$ , where

$$E_\nu(x) = \sum_{r=0}^{\infty} \frac{x^r}{\Gamma(1+r\nu)}, \quad x, \nu \in \mathbb{C}, \quad \Re(\nu) > 0.$$

**Remark 3.3.** Note that, when the fractional-order  $\nu = 1$ , Definitions 3.1 and 3.2 reduce to the classical Definitions of integral and differential.

So, the generalized model (2.1) in the setting

of ABC-fractional derivative is of the form

$$\begin{aligned} {}^{ABC}\mathcal{D}_{0^+}^\nu S(t) &= \mathcal{H}_1(t, S(t)), \\ {}^{ABC}\mathcal{D}_{0^+}^\nu E(t) &= \mathcal{H}_2(t, E(t)), \\ {}^{ABC}\mathcal{D}_{0^+}^\nu A(t) &= \mathcal{H}_3(t, A(t)), \\ {}^{ABC}\mathcal{D}_{0^+}^\nu Q(t) &= \mathcal{H}_4(t, Q(t)), \\ {}^{ABC}\mathcal{D}_{0^+}^\nu I(t) &= \mathcal{H}_5(t, I(t)), \\ {}^{ABC}\mathcal{D}_{0^+}^\nu R(t) &= \mathcal{H}_6(t, R(t)), \end{aligned} \quad (3.1)$$

where the kernels are given by

$$\begin{aligned} \mathcal{H}_1(t, S(t)) &= \Lambda - \eta\kappa S - \mu S, \\ \mathcal{H}_2(t, E(t)) &= \eta\kappa S - (\sigma_1\tau_2 + \sigma_2\alpha_1 + \mu + \tau_1 \\ &\quad - \sigma_1\tau_1 - \sigma_2\tau_1)E, \\ \mathcal{H}_3(t, A(t)) &= \sigma_1\tau_2 E - (r_1 + \mu)A, \\ \mathcal{H}_4(t, Q(t)) &= \sigma_2\alpha_1 E - (\sigma_3\alpha_2 + r_2 - r_2\sigma_3 + \mu)Q, \\ \mathcal{H}_5(t, I(t)) &= (1 - \sigma_1 - \sigma_2)\tau_1 E + \sigma_3\alpha_2 Q \\ &\quad - (r_3 + \mu + \delta)I, \\ \mathcal{H}_6(t, R(t)) &= r_1 A + (1 - \sigma_3)r_2 Q + r_3 I - \mu R, \end{aligned} \quad (3.2)$$

where  ${}^{ABC}\mathcal{D}_{0^+}^\nu(\cdot)$  is the ABC-fractional derivative of order  $(0 < \nu \leq 1)$  with nonnegative variables and subjected to suitable initial conditions.

Applying the fractional operator  ${}^{ABC}I_{0^+}^\nu$ , to both sides of system (3.1), we have a system of an integral equation given by

$$\begin{aligned} S(t) - S(0) &= {}^{ABC}I_{0^+}^\nu \mathcal{H}_1(t, S(t)), \\ E(t) - E(0) &= {}^{ABC}I_{0^+}^\nu \mathcal{H}_2(t, E(t)), \\ A(t) - A(0) &= {}^{ABC}I_{0^+}^\nu \mathcal{H}_3(t, A(t)), \\ Q(t) - Q(0) &= {}^{ABC}I_{0^+}^\nu \mathcal{H}_4(t, Q(t)), \\ I(t) - I(0) &= {}^{ABC}I_{0^+}^\nu \mathcal{H}_5(t, I(t)), \\ R(t) - R(0) &= {}^{ABC}I_{0^+}^\nu \mathcal{H}_6(t, R(t)), \end{aligned} \quad (3.3)$$

upon simplification yields

$$\begin{aligned} S(t) &= S(0) + \Psi(\nu)\mathcal{H}_1(t, S(t)) \\ &\quad + \Phi(\nu) \int_0^t (t-x)^{\nu-1} \mathcal{H}_1(x, S(x)) dx, \\ E(t) &= E(0) + \Psi(\nu)\mathcal{H}_2(t, E(t)) \\ &\quad + \Phi(\nu) \int_0^t (t-x)^{\nu-1} \mathcal{H}_2(x, E(x)) dx, \\ A(t) &= A(0) + \Psi(\nu)\mathcal{H}_3(t, A(t)) \\ &\quad + \Phi(\nu) \int_0^t (t-x)^{\nu-1} \mathcal{H}_3(x, A(x)) dx, \end{aligned}$$

$$\begin{aligned}
 Q(t) &= Q(0) + \Psi(v)\mathcal{H}_4(t, Q(t)) \\
 &\quad + \Phi(v) \int_0^t (t-x)^{v-1} \mathcal{H}_4(x, Q(x)) dx, \\
 I(t) &= I(0) + \Psi(v)\mathcal{H}_5(t, I(t)) \\
 &\quad + \Phi(v) \int_0^t (t-x)^{v-1} \mathcal{H}_5(x, I(x)) dx, \\
 R(t) &= R(0) + \Psi(v)\mathcal{H}_6(t, R(t)) \\
 &\quad + \Phi(v) \int_0^t (t-x)^{v-1} \mathcal{H}_6(x, R(x)) dx,
 \end{aligned} \tag{3.4}$$

where

$$\Psi(v) = \frac{1-v}{\Gamma(v)}, \quad \Phi(v) = \frac{v}{\Gamma(v)} \frac{1}{\Gamma(v)}.$$

### 3.1 Existence and uniqueness results

Fixed point theorems play a vital role in establishing the existence and uniqueness of solutions of the nonlinear fractional differential equation. In this subsection, utilizing the techniques of Schaefer's and Banach's fixed point theorem, we establish the existence and uniqueness of solutions of the fractional model (3.1). Re-writing the model (3.1) as:

$$\begin{cases} {}^{ABC}\mathcal{D}^v \Theta(t) = \mathcal{H}(t, \Theta(t)), \\ \Theta(0) = \Theta_0, \quad 0 < t < T < \infty. \end{cases} \tag{3.5}$$

The vector  $\Theta(u) = (S, E, A, Q, I, R)^T$  and  $\mathcal{H}(\cdot)$  in (3.5) represent the state variables and a continuous vector function respectively defined as follows:

$$\mathcal{H} = (\mathcal{H}_1, \mathcal{H}_2, \mathcal{H}_3, \mathcal{H}_4, \mathcal{H}_5, \mathcal{H}_6)^T, \tag{3.6}$$

with initial conditions

$$\Theta_0(t) = (S(0), E(0), A(0), Q(0), I(0), R(0)).$$

Corresponding to (3.5), the integral equation is given by

$$\begin{aligned}
 \Theta(t) &= \Theta_0 + \Psi(v)\mathcal{H}(t, \Theta(t)) \\
 &\quad + \Phi(v) \int_0^t \mathcal{H}(x, \Theta(x))(t-x)^{v-1} dx.
 \end{aligned} \tag{3.7}$$

#### 3.1.1 Existence results

Consider  $\mathcal{A} = [0, T]$ ,  $\mathcal{M} = C(\mathcal{A}, \mathbb{R}^6)$  and the Picard operator  $\mathcal{F} : \mathcal{M} \rightarrow \mathcal{M}$  be given by

$$\begin{aligned}
 \mathcal{F}[\Theta(t)] &= \Theta_0 + \Psi(v)\mathcal{H}(t, \Theta(t)) \\
 &\quad + \Phi(v) \int_0^t \mathcal{H}(x, \Theta(x))(t-x)^{v-1} dx.
 \end{aligned} \tag{3.8}$$

Together with the supremum norm  $\|\cdot\|_C$ , on  $\Theta$  is defined by

$$\|\Theta(t)\|_{\mathcal{M}} = \sup_{t \in \mathcal{A}} \|\Theta(t)\|, \quad \Theta(t) \in \mathcal{M}, \tag{3.9}$$

$\mathcal{M}$  defines a Banach space. Assume the following

$\mathcal{B}_1$ . Let  $\mathcal{H} : A \times \mathbb{R}^6 \rightarrow \mathbb{R}^6$  is continuous.

$\mathcal{B}_2$ . There exists  $C_{\mathcal{H}} > 0$  such that  $|\mathcal{H}(t, \Theta) - \mathcal{H}(t, \Theta')| \leq C_{\mathcal{H}}|\Theta - \Theta'|$ , for all  $\Theta, \Theta' \in \mathbb{R}^6$ .

$\mathcal{B}_3$ . There exists a constant  $L > 0$  such that  $|\mathcal{H}(x, \Theta)| \leq L(1 + |\Theta|)$  for each  $x \in A$  and all  $\Theta \in \mathbb{R}^6$ .

Now, we use Schaefer's fixed point theorem to prove the existence of at least one solutions of the problem (3.5).

**Theorem 3.4.** Assume the hypotheses  $[\mathcal{B}_1]$ - $[\mathcal{B}_3]$  together with  $1 - \Psi(v)L > 0$ , holds. Then the exists at least one solution of problem (3.5) which is equivalent with the fractional model (3.1).

#### 3.1.2 Uniqueness Result

We now show by using Banach contraction principle that the solution of (3.5) is unique.

**Theorem 3.5.** Assuming  $\mathcal{B}_1 - \mathcal{B}_2$  together with

$$\left( \Psi(v) + \frac{\Phi(v)T^v}{v} \right) C_{\mathcal{H}} < 1,$$

then there exists a unique solution of (3.5) which is equivalent with the fractional model (3.1).

## 4. Model Fitting and Base Line Parameters

Validation of a newly established epidemiological model is one of the important mechanisms for the study of disease transmission dynamics. The availability of real data on the underlying disease greatly contributes to the completion of this mission. And the actual data gives us an insight into how to assess the best values of such unknown biological parameters involved in the model. To this purpose, nonlinear least-squares curve fitting method with the help of the "fminsearch" function from the MATLAB Optimization Toolbox were employed to do the job. This approach states that, if a theoretical model  $t \mapsto \Xi(t, q_1, q_2, \dots, q_n)$  is attained and depends on a few unknown parameters  $q_1, q_2, \dots, q_n$  and a sequence of actual data points  $(t_0, y_0), \dots, (t_j, y_j)$  is also at hand then the aim is to obtain values of the parameters so that the error calculated can,

$$E := \sqrt{\sum_{i=0}^j \left( \Xi(t, q_1, q_2, \dots, q_n) - y_i \right)^2}, \tag{3.5}$$

attain a minimum. The following parameters  $\mu, \eta, \xi_{se}, \xi_{sa}, \xi_{sa}, \alpha_2, \sigma_3, r_1, r_2, r_3$  and  $\delta$  have been best fitted, while the parameters  $\Lambda, \sigma_1, \sigma_2, \alpha_1, \tau_1$  and

$\tau_2$  have been assumed as displayed in Table 3 and Fig. 7, respectively. The initial conditions for the state variables are  $S(0) = 26690$ ,  $E(0) = 4820$ ,  $A(0) = 9398$ ,  $Q(0) = 1321$ ,  $I(0) = 1795$  and  $R(0) = 793$ .

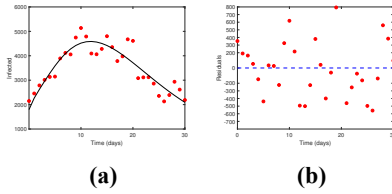


**Fig. 7.** The daily COVID-19 cumulative cases time series in Turkey from 1 July to July 31, 2020 with the best fitted curve from simulations of the proposed model and (b) the residuals for the best fitted curve.

**Table 3.** Estimation of the parameters values.

| Parameters | Value   | Source |
|------------|---------|--------|
| $\mu$      | 0.0056  | Fitted |
| $\eta$     | 0.60107 | Fitted |
| $\xi_{se}$ | 0.18566 | Fitted |
| $\xi_{sa}$ | 0.51428 | Fitted |
| $\xi_{si}$ | 0.41136 | Fitted |
| $\sigma_1$ | 0.2     | [25]   |
| $\sigma_2$ | 0.1496  | [25]   |
| $\alpha_1$ | 0.0998  | [25]   |
| $\tau_1$   | 0.2     | [25]   |
| $\tau_2$   | 0.1496  | [25]   |
| $\alpha_2$ | 0.65200 | Fitted |
| $\sigma_3$ | 0.40822 | Fitted |
| $r_1$      | 0.09823 | Fitted |
| $r_2$      | 1.24484 | Fitted |
| $r_3$      | 0.14835 | Fitted |
| $\delta$   | 0.00367 | Fitted |

#### 4.1 Iterative scheme and graphical analysis

Here, we used the recent and effective numerical scheme proposed by Toufik and Atangana in [26]. For the detailed analysis of the convergence, accuracy, and stability of the method, see [26]. Using the baseline values of the parameters as displayed in Table 3, we simulate the proposed COVID-19 model for both classical and fractional order deriva-

tives which shows the dynamic trajectories of each of the compartment.

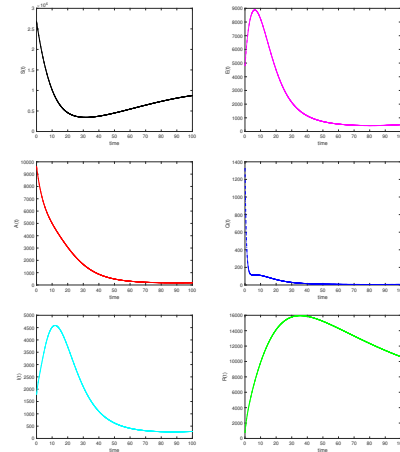


**Fig. 8.** Profiles for behavior of each state variable for the classical version of the model.

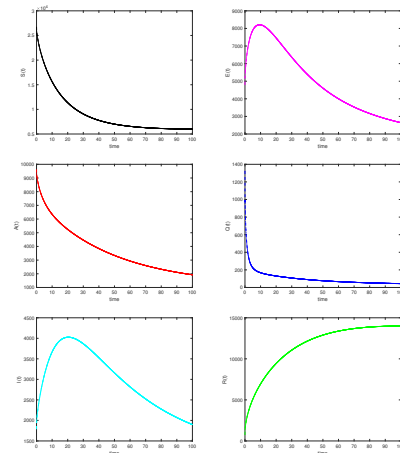


**Fig. 9.** Profiles for behavior of each state variable for the ABC version of the fractional model.

In Figs. 8-9, we present the dynamics trajectories of the state variables for classical and ABC version respectively, which shows strong correlations between the integer and non-integer case. To push the epidemic investigation one step further, we vary the fractional-order for different values of  $\nu = 1, 0.95, 0.85, 0.75, 0.65$ , which shows clearly the effect of the fractional-order as shown in Fig. 10. The impacts of  $\nu$  are even more pronounced for example; in Figure 10(a), a decrease of the fractional-order  $\nu$



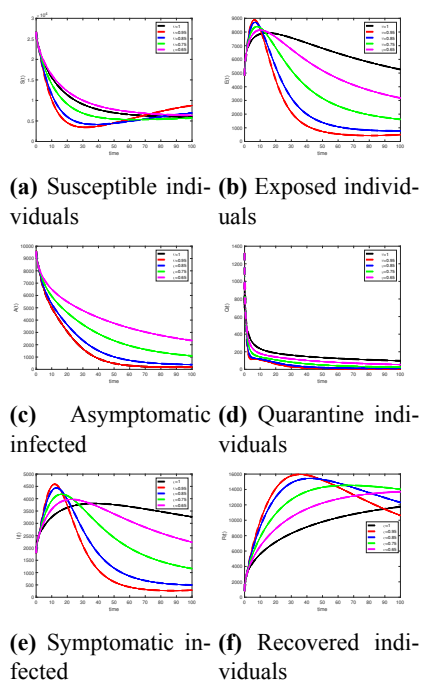


**Fig. 10.** Comparison of each state variables for classical and fractional order.

leads to the decrease and increase of the number of the susceptible individual in the populations. Similarly, from 0-10 days, the number of exposed individuals increases and then starts decreasing and becomes stable as displayed in Fig. 10(b). An interesting scenario occurs in the asymptomatic infected and quarantined compartment which shows the decrease of the fractional-order leads to the decrease of each of the compartments as shown in Figs. 10(c)-10(d). Furthermore, we observe the significant reduction in the number of recovered infected individuals who are symptomatic and the increase of the number of recovered individuals for smaller fractional orders as shown in Figs. 10(e)-10(f). In this regard, it will be interesting to see various properties of the dynamic pattern of the COVID-19 model with different fractional-order ( $0 < \nu < 1$ ) compared with the integer case  $\nu = 1$ .

## 5. Conclusions

In this paper, we study a mathematical model to analyze the transmission patterns of the novel Coronavirus (COVID-19) using publically available data. We show that the disease free equilibrium is locally asymptotically stable when  $R_0 < 1$ . Besides,

for more accurate, realistic, and precise short-term predictions, we generalized the model to fractional-order derivative in the sense of the ABC fractional operator. We provided a computational scheme for the solution of the fractional model and reported different graphical results. Decreasing the fractional-order parameters leads to a decrease in infection in the infected compartments. The analysis result suggests that quarantine is the most powerful non-pharmaceutical measure to monitor the mechanisms of the spread of the emerging coronavirus disease (COVID-19), which has badly affected the world as a whole. The findings presented can be useful in identifying the ongoing pandemic more comprehensively and may help to reduce the outbreak to a minimum by taking precautionary steps.

## Acknowledgment

The authors express their gratitude for the positive comments received by anonymous reviewers and the editor which led to an extensive improvement of the manuscripts. These works were done while the first author visits Cankaya University, Ankara, Turkey.

## Availability of data and material

All data used in this analysis can be assessed via [www.worldometers.info-coronavirus-country-turkey](http://www.worldometers.info-coronavirus-country-turkey).

## References

- [1] Wege H, Ter Meulen V, et al. The biology and pathogenesis of coronaviruses. 1982; 165-200.
- [2] Kahn JS, McIntosh K. History and recent advances in coronavirus discovery. The Pediatric infectious disease journal. 2005;24(11): S223-7.
- [3] Zhu N, Zhang D, Wang W, Li X, Yang B, Song J, et al. A novel coronavirus from patients with pneumonia in China, 2019. New England Journal of Medicine. 2020;382(8):727-33.
- [4] Li Q, Guan X, Wu P, Wang X, Zhou L, Tong Y, et al. Early transmission dynamics in Wuhan, China, of novel coronavirus-infected pneumonia. New England Journal of Medicine. 2020;382(13):1199-207.

- [5] Rihan FA; Hindawi. Numerical modeling of fractional-order biological systems. 2013;2013.
- [6] Podlubny I. Fractional differential equations: an introduction to fractional derivatives, fractional differential equations, to methods of their solution and some of their applications. vol. 198. Elsevier; 1998.
- [7] Kilbas A, Srivastava H, Trujillo J. Theory and Applications of fractional differential Equations. North-Holland Mathematics Studies. 2006;204.
- [8] Atangana A. Derivative with a new parameter: Theory, methods and applications. Academic Press; 2015.
- [9] Atangana A. Fractional operators with constant and variable order with application to geo-hydrology. Academic Press; 2017.
- [10] Caputo M, Fabrizio M. A new definition of fractional derivative without singular kernel. Progr Fract Differ Appl. 2015;1(2):1-13.
- [11] Atangana A. Non validity of index law in fractional calculus: A fractional differential operator with Markovian and non-Markovian properties. Physica A: Statistical Mechanics and its Applications. 2018;505:688-706.
- [12] Safare KM, Betageri VS, Prakasha DG, Veerasha P, Kumar S. A mathematical analysis of ongoing outbreak COVID-19 in India through nonsingular derivative. Numerical Methods for Partial Differential Equations. 2021;37:1282-98.
- [13] Ali KK, Abd El Salam MA, Mohamed EM, Samet B, Kumar S, Osman M. Numerical solution for generalized nonlinear fractional integro-differential equations with linear functional arguments using Chebyshev series. Advances in Difference Equations. 2020;2020(1):1-23.
- [14] Khan MA, Atangana A. Modeling the dynamics of novel coronavirus (2019-nCov) with fractional derivative. Alexandria Engineering Journal. 2020;59(4):2379-89.
- [15] Zhang Z. A novel COVID-19 mathematical model with fractional derivatives: singular and nonsingular kernels. Chaos, Solitons & Fractals. 2020;139:110060.
- [16] Khan MA, Atangana A, Alzahrani E, et al. The dynamics of COVID-19 with quarantined and isolation. Advances in Difference Equations. 2020;2020(1):1-22.
- [17] Ahmed I, Baba IA, Yusuf A, Kumam P, Kumam W. Analysis of Caputo fractional-order model for COVID-19 with lockdown. Advances in Difference Equations. 2020;2020(1):1-14.
- [18] Baba IA, Nasidi BA. Fractional order epidemic model for the dynamics of novel COVID-19. Alexandria Engineering Journal. 2020;60(1):537-48.
- [19] Goufo EFD, Khan Y, Chaudhry QA. HIV and shifting epicenters for COVID-19, an alert for some countries. Chaos, Solitons and Fractals. 2020;139:110030.
- [20] worldometers.info;  
<https://www.worldometers.info/coronavirus/country/turkey/>.
- [21] Van den Driessche P, Watmough J. Further notes on the basic reproduction number. In: Mathematical epidemiology. Springer; 2008. p. 159-78.
- [22] Atangana A, Baleanu D. New fractional derivatives with nonlocal and non-singular kernel: Theory and application to heat transfer model. Thermal Science. 2016;20(2):763-9.
- [23] Ahmed I, Modu GU, Yusuf A, Kumam P, Yusuf I. A Mathematical Model of Coronavirus Disease (COVID-19) Containing Asymptomatic and Symptomatic Classes. Results in Physics;p. 103776.
- [24] Akgul A. A novel method for a fractional derivative with non-local and non-singular kernel. Chaos, Solitons & Fractals. 2018;114:478-82.
- [25] Jia J, Ding J, Liu S, Liao G, Li J, Duan B, et al. Modeling the control of

COVID-19: Impact of policy interventions and meteorological factors. arXiv preprint arXiv:200302985. 2020;23:1-24.

- [26] Toufik M, Atangana A. New numerical approximation of fractional derivative with non-local and non-singular kernel: application to chaotic models. The European Physical Journal Plus. 2017;132(10):444.